



THE UNIVERSITY OF KANSAS SPACE TECHNOLOGY CENTER  
Raymond Nichols Hall CENTER FOR RESEARCH, INC.

2291 Irving Hill Drive—Campus West Lawrence, Kansas 66045

Telephone:

NASA CR.

NASA CR.

140 314

S-193 SCATTEROMETER TRANSFER FUNCTION  
ANALYSIS FOR DATA PROCESSING

CRES Technical Report 236-2

Leland Johnson

(NASA-CR-140314) S-193 SCATTEROMETER  
TRANSFER FUNCTION ANALYSIS FOR DATA  
PROCESSING (Kansas Univ. Center for  
Research, Inc.) 19 p HC \$3.25 CSCL 14B

N75-10569

Unclas

G3/43 53184

July, 1974

**PRICES SUBJECT TO CHANGE**

Supported by:

NATIONAL AERONAUTICS AND SPACE ADMINISTRATION

Lyndon B. Johnson Space Center

Houston, Texas 77058

CONTRACT NAS 9-13347

Reproduced by  
NATIONAL TECHNICAL  
INFORMATION SERVICE  
US Department of Commerce  
Springfield, VA. 22151

## ABSTRACT

This technical report analyzes a mathematical model for converting raw data measurements of the S-193 scatterometer into processed values of radar scattering coefficient. The argument is based on an approximation derived from the Radar Equation and actual operating principles of the S-193 Scatterometer hardware. Possible error sources are inaccuracies in transmitted wavelength, range, antenna illumination integrals, and the instrument itself. The dominant source of error in the calculation of scattering coefficient is accuracy of the range. All other factors with the possible exception of illumination integral are not considered to cause significant error in the calculation of scattering coefficient.

11

## 1.0 INTRODUCTION

This technical report defines conversion of raw S-193 scatterometer measurements and ephemeris data into processed values of radar scattering coefficient. This is accomplished by reviewing fundamental operation of the S-193 scatterometer receiver circuitry, developing the scattering coefficient from the radar equation, and finally relating scatterometer voltage measurements to complete calculation of the scattering coefficient. Although the purpose of this report does not include numerical determination of any system parameter, this report will define expected areas of difficulty with accurate determination of all system parameters. Since the data analyzed to date has not shown behavior consistent with gross system parameter errors, the represented calculation of scattering coefficient is considered valid.

## 2.0 S-193 SCATTEROMETER OPERATION

The S-193 is actually three instruments: an altimeter, a radar scatterometer, and a microwave radiometer. The major system modes are ALTIMETER, SCATTEROMETER ONLY, RADIOMETER ONLY, and RADIOMETER/SCATTEROMETER. A 13.9 GHz pulsed CW transmitter is common to the altimeter and scatterometer, and the receiver front end is common to all three systems. SCAT CALIBRATION, RAD CALIBRATION, and RAD BASELINE signals, however, are injected at different points in the receiver front end.

After the first frequency down-conversion to 500 MHz (BW=20 MHz), the filtered IF is split in a three-way power divider to the altimeter, the rad processor, and the scat processor. Inside the scat processor, the signal is down-converted again to 50 MHz (BW=2MHz), and the filtered IF is passed through a bank of electronically selectable 10 dB attenuation steps. This increases scatterometer dynamic range to more than 40 dB, although as many as three scat pulses may be lost due to reprogramming the attenuators to keep filter output within the dynamic limit of the instrument. After further amplification, the signal is gated into one of five doppler filter banks according to the current pitch command angle of the antenna scan. The exception to this rule is the SCAT CAL measurement which must go through the unshifted doppler filter bank at 0° pitch.

/

Each filter bank consists of an upper, middle, and lower center frequency filter. The bandwidths overlap to provide complete coverage of the received sea signal with small bandwidth. This smaller bandwidth lowers noise energy and improves signal resolution in the presence of noise. The upper, middle, and lower center frequency filters for the five pitch command angles are next reassembled in three five-way power combiners. These three signal channels are separately amplified, detected, and integrated over the measurement period. The outputs of the three integrators are encoded in the DHCU, and the largest signal is selected as the measurement to be recorded as a data point. Hanley<sup>1</sup> provides a more detailed discussion of system operation.

Actual measurement timing parameters (integration time) and integrator configuration (time constant) are dependent on scan mode and measurement type. A tabulation of these values as well as a scan description for each mode is given in the GE Calibration Data Report, Vol. 1A. The "best estimates" of system parameters, i.e. most recently accepted values, are contained in the EREP Sensor Performance Report Volume IV (S-193 R/S).

### 3.0 CALCULATION OF SCATTERING COEFFICIENT

#### 3.1 Radar Equation

The scattering coefficient is calculated by applying the Radar Equation for a single antenna CW scatterometer system:<sup>2</sup>

$$P_r = \frac{P_t \lambda^2}{(4\pi)^3} \int_A \frac{G_r G_t \sigma^0}{R^4} dA \quad (1)$$

<sup>1</sup>W. R. Hanley, Analysis of S-193 Microwave Rad/Scat for Skylab, Ph.D Dissertation, Chapter 4.

<sup>2</sup>R. K. Moore, The Radar Handbook, p. 25-16 ff., McGraw-Hill, 1970

$P_r$  = power received at the antenna  
 $P_t$  = power radiated from the antenna  
 $\lambda$  = transmitter wavelength  
 $G_r$  = normalized antenna gain pattern for the received signal  
 $G_t$  = normalized antenna gain pattern for the transmitted signal  
 $R$  = one-way radar range  
 $A$  = illuminated area  
 $\sigma^0$  = scattering coefficient

Equation (1) does not strictly apply to the S-193 Scatterometer, since the transmitter RF is pulse modulated (125 pps) with a 62.5% duty cycle. There are additional modulation timing constraints which depend upon system mode, but these timing constraints are of much longer period than the basic pulse repetition frequency. Since the operating frequency of the radar is 13.9 GHz, the modulation sidebands are so small that transmitter wavelength is accurately approximated by a constant. In addition, equation (1) is used for propagation through a lossless medium. Calculation of atmospheric losses in general requires meteorological data and a knowledge of the physical interaction mechanisms involved. It was therefore determined to process the data assuming lossless propagation, and to consider any atmospheric effects separately in the form of an insertion loss.

Equation (1) is now simplified according to Moore<sup>3</sup> by treating the scattering coefficient as a constant over the illuminated area, and ignoring variations in range over the illuminated area. The actual vehicle altitude and antenna patterns taken during preflight testing by GE support the validity of these simplifying assumptions, but the KU Skylab APEX results should be checked to strengthen this argument. The APEX results for SL-4 are crucial, since the radiated pattern was clearly different from the field data of SL-2 and SL-3. This task, however, is the objective of a separate investigation and bears upon processing of SL-4 data only.

With these simplifications, Equation (1) is now solved for the scattering coefficient:

$$\sigma^0 \approx \frac{(4\pi)^3 R^4}{\lambda^2} \left( \frac{P_r}{P_t} \right) \frac{1}{\int_A G_r G_t dA} \quad (2)$$

---

<sup>3</sup> op. cit. p. 25-16.

Since the S-193 scatterometer may transmit and receive two different polarizations, the illumination integral in Equation (2) has four values which depend on system polarization mode:  $I_{HH}$ ,  $I_{HV}$ ,  $I_{VH}$ ,  $I_{VV}$ . The subscripts V and H refer to the selection of one travelling wave polarization from two orthogonal waveguide modes, and have no significance with respect to the earth's surface. The first subscript refers to transmit polarization, and the second refers to receiver polarization. The values of these integrals were computed from GE preflight test data, and will be checked again when the KU APEX analysis is complete. The range in Equation (2) is computed from ephemeris data assuming a spherical earth, using the S-193 pitch and roll gimbal angles. Wavelength is calculated from preflight measurements of transmitter frequency. SCAT calibration measurements in space are used to check stability of transmitter frequency by using two overlapping doppler filters from the  $0^\circ$  pitch filter bank in the two SCAT CAL measurements. It remains to calculate the measurement of  $(P_R/P_T)$  by the instrument.

### 3.2 Modeling the S-193 Scatterometer

The measurement quantities of the scatterometer are SCAT (signal plus noise), SCAT NOISE (noise only), and SCAT CAL (calibration signal) voltages. Since these voltages represent quantities which have been square-law detected, they are actually power measurements. In order to calculate the ratio of received to transmitted power, the signal paths of the measured quantities must be normalized with respect to each other. The normalized measurements must then be corrected for the integration and analogue/digital conversion processes. The processed numbers may now be directly compared to compute the  $(P_R/P_T)$  ratio for the backscattering coefficient calculation.

#### 3.2.1 Measurement Normalization

SCAT and SCAT NOISE signals always share a common path from the antenna to the A/D Converter with the exception of the Gain Selection network. This network is a set of four 10 db attenuation steps used to improve linearity and boost dynamic range of the instrument. Addition of the appropriate number of db by noting the attenuator selected will allow direct comparison of SCAT and SCAT NOISE voltages for a given operating mode. To compare values of these measured quantities, however, requires further calculation.

4

The measured values of SCAT and SCAT NOISE power were obtained using different integration times. After normalization, it is apparent that the result is an average SIGNAL PLUS NOISE power and NOISE power for the entire measurement period. If the signal and noise processes are not correlated, i.e. orthogonal, then the signal may be recovered by subtracting the normalized SCAT NOISE voltage from the normalized SCAT measurement. Thus, a measure of signal power in the radar return is defined.

The SCAT CAL measurements are used to determine transmitted power at the antenna plane. By inserting a known value of attenuation in the receiver path while the transmitter is operating, transmitter output power can be determined. Since the S-193 scatterometer design scaled the SCAT CAL amplitude to the top of the dynamic range of the instrument, system noise is more than 40 db down from the signal. For this reason, noise in the SCAT CAL measurement is ignored. It should be pointed out that transmitter output power is assumed to be time-invariant between SCAT CAL measurements (~4 minutes). Preflight testing and space data support this assumption; total variations of valid SCAT CAL measurements in SL-2, SL-3, and SL-4 were less than 1 db. This conforms to the requirement on desired accuracy of the scattering coefficient.

Two further considerations are required prior to comparison of SCAT minus SCAT NOISE and SCAT CAL measurements. The first consideration requires path normalization for the S-193 receiver front end, and the second requires path normalization for the SCAT processor. The model of the receiver front end is shown in Figure 3.2.1-1.

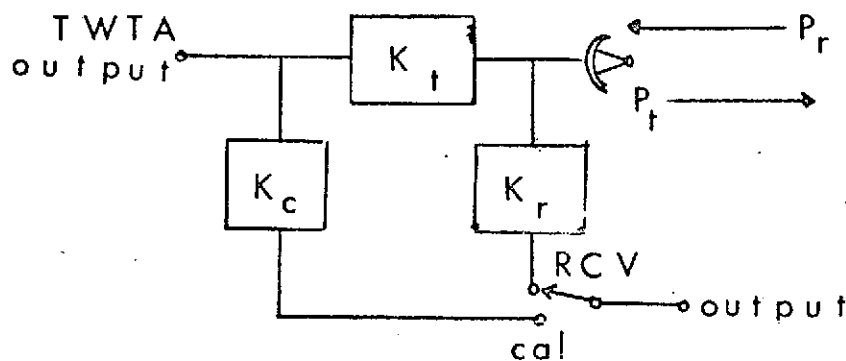


Figure 3.2.1-1.

5

$P_R$  = power received at the antenna  
 $P_T$  = power transmitted from the antenna  
 $K_T$  = loss common between antenna and TWTA  
 $K_C$  = loss (attenuation) in calibration  
 $K_R$  = loss common to the receive path

If these loss coefficients are indeed constant, then the ratio of received power to transmitted power may be computed. This is done by defining TWTA output as  $P_T/K_T$ , and realizing that the front-end output is anywhere in the scat receiver path between the D circulator and the attenuator bank. The OUTPUT point, however, is only a computational aid, since any such point in the real scat receiver will be contaminated with broad band noise. Since it has been previously assumed that the noise can be successfully decoupled, however, the received power can be taken as a clean signal in Figure 3.2.1-1 for the purposes of calculation.

The ratio of a signal to calibration measurement at the OUTPUT terminal is therefore

$$\frac{V_s}{V_c} = \frac{P_k K_r}{P_t K_c} = \frac{K_t K_r}{K_c} \left( \frac{P_r}{P_t} \right) \quad (3)$$

or alternately,

$$\frac{P_r}{P_t} = \frac{K_c}{K_t K_r} \frac{V_s}{V_c} \quad (3a)$$

$V_s$  = ideal noise-free voltage received

$V_c$  = ideal calibration voltage measured

In addition to considering path normalization inside the scat processor, it should be mentioned that all signals are narrow-band filtered to minimize noise power. This is less important for the SCAT CAL measurement due to the relative magnitudes of signal and noise. The difficulty with the signal measurement, however, is the doppler shifting and doppler spreading of the return spectrum. This is caused by relative motion of the Skylab vehicle with respect to the earth and finite beamwidth of the antenna.

6



The ideal solution to this problem would be a single filter whose passband and center frequency track pitch and roll gimbal angles together with known attitude of the OWS (with respect to the earth). This design would perfectly match the return spectrum and minimize noise power. Such a filter is not as practical for obvious technical reasons. Advances in state-of-the-art, however, may solve the technical problems and implement this method in future generations of scatterometers.

What can be done, however, is to construct a bank of selectable filters with large overlapping bandwidths to cover all expected center frequency doppler shifts for the entire scan range of the instrument. Three overlapping filters for each pitch command angle were used for this purpose, selecting the largest filter output as representative of the signal plus noise power. This concept will introduce some imprecision over the ideal single tracking filter, but the degradation has not been serious. Since the signal plus noise measurement and the noise-only measurement are taken with the same filter, there is no apparent conflict in resolving the signal if the noise and signal processes are uncorrelated.

There will be a conflict, however, in comparing any two scatterometer signal measurements (after subtracting the noise) in general. Normalization of all measurements should be accomplished with respect to the doppler bandwidth and not filter bandwidth. This difficulty was resolved by constructing filter bandwidths proportional to expected doppler bandwidths for the five discrete pitch command angles. All measurements may now be normalized with respect to the input of the three signal integrators.

Equation (3a) showed the ratio of received to transmitted power to be directly proportional to the ratio of "clean" signal voltage to an ideal calibration voltage. The actual ratio found from the measured voltages is computed by first subtracting the noise power from the signal plus noise power and then normalizing the result to the calibration measurement. This is not really possible, since all measurements are time-averaged by integration. On the other hand, an instantaneous value of scattering coefficient is of little practical value due to the statistics of noise.

### 3.2.2 Integration Normalization

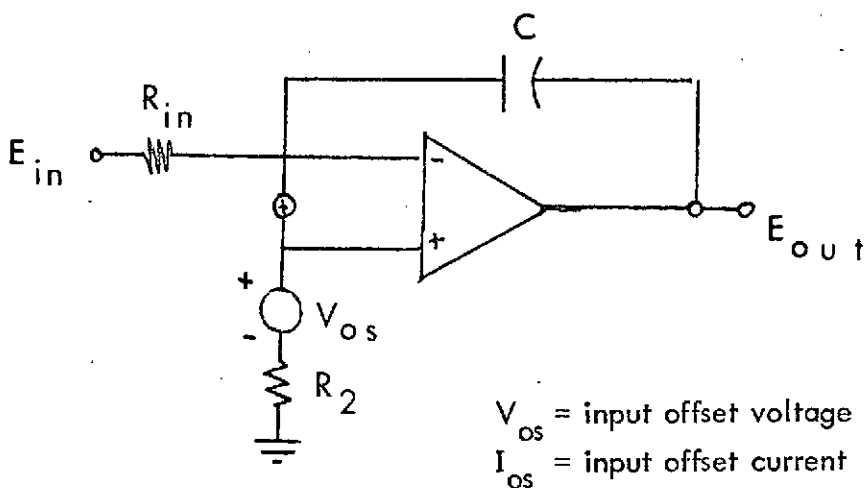
It has been shown in the previous section that the only differences between the voltages at the inputs of the three integrators are due to different 10 db attenuation steps and the narrow-banded doppler filters. Since these processing mechanisms are electronically controlled, it is possible to monitor the electronic configuration of the

of the Scat Processor and to use this information in the data processing. The final processes applied to each measurement are square law detection, amplification, integration, and A/D conversion.

Linearity of the detection and amplification processes well into the noise floor of the instrument was established in preflight testing.<sup>4</sup> By measuring the linear coefficient for each data channel, these processes could be lumped into the filter gains. Not so easily accomplished, however, is the modeling of the integrators.

The general model of an analogue integrator is shown in Figure 3.2.2-1. This model is not a

Figure 3.2.2-1



detailed representation, since finite gain, bandwidth, input offset current, input and output impedance effects have been neglected. The usual justifications in neglecting these quantities are an orders-of-magnitude comparison and judicious choice of the operating envelope.

There is a minor difficulty in neglecting the input offset current. Usual design practice is to make  $R_{in} = R_2$  in the integrator circuit of Figure 3.2.2-1. By assuming identical transistors in the differential input stage, the offset current due to bias errors is forced to zero. In the Scat processor, however, there are three distinct time constants formed by changing the value of  $R_{in}$ . The mismatch of  $R_{in}$  to  $R_2$  will introduce a small offset current error, which will be integrated during the measurement interval.

<sup>4</sup> GE Historical Logbook, Volume 5, p. 272-275.

8

In addition, the input offset voltage  $V_{os}$  will appear at the output immediately after beginning the integration, and the output will ramp according to the  $\frac{R_{in} C}{RC}$  time constant and integration time. Expressing these effects quantitatively,

$$e_o = e_{in} \left( \frac{t}{R_{in} C} \right) + V_{os} \left( 1 + \frac{t}{R_{in} C} \right) + I_{os} \left( \frac{t}{C} \right) \quad (4)$$

$e_o$  = output voltage

$e_{in}$  = input voltage

$V_{os}$  = input offset voltage

$I_{os}$  = input offset current

$R_{in}$  = integration time constant resistor

$C$  = integration time constant capacitor

$t$  = integration time

It can be seen from Equation (4) that the output voltage contains a dc error term as well as a ramp error voltage. In order to reconstruct the true output voltage resulting from the input signal, these two error terms must be measured. This could have been implemented as a periodic calibration measurement by grounding the input terminal, but it was decided to treat the offset errors as quantities depending only upon temperature. Similar argument was made for the filter gain numbers, but here the major temperature contribution resulted from the detector diodes.

It might be felt that this treatment of offset errors is oversimplified and incomplete. On the other hand, there has been ample evidence in the SCAT NOISE data from space to indicate that the processed SCAT NOISE measurement is virtually independent of mode and command angle. It may be therefore concluded that the offset errors measured during preflight testing are appropriate.

### 3.2.3 Analogue to Digital Conversion

Preceding sections of this report have indicated normalization procedures necessary to directly compare any two scat measurements. It was also mentioned that the output of the three data channels are compared in the DHCU, and the largest output becomes the recorded measurement. The only exceptions to this rule are the scat noise measurement (which uses the same data channel as the preceding Scat measurement), and the Scat cal measurements (where the data channel is preselected).

The A/D converter in the scat processor is a 10-bit successive approximation device. Successive approximation conversion is a fixed conversion rate process where the input is successively compared with a digital level. Beginning with the most significant bit (MSB), the A/D output register is set to  $(1000000000)_2$ . If the comparison shows the analogue signal is larger than the output register, the MSB is kept at logical one and the next most significant bit is set to one for the second comparison. Should the result of the original comparison indicate the digital register voltage was larger than the analog input (notice that this method requires a D/A converter to form the analogue of the digital register voltage), the MSB is set to logical zero and the second most significant bit is set to logical one for the next comparison. The process is complete when the least significant bit (LSB) has been determined, or after ten successive approximations.

Typical problems with this conversion method are resolution, linearity, hysteresis, and temperature effects. Comparator offset and D/A conversion are the major sources of error and are usually responsible for the limiting resolution of an A/D converter. It was originally proposed to account for all non-linear behavior by building a calibration table for each A/D measurement mode.<sup>5</sup> Subsequent data analysis has shown that this approach induces significantly more data scatter over a homogeneous target than assuming a perfectly linear conversion, i. e. bit calibration weights of  $2^{-N}$  volts, where N is one for the MSB and ten for the LSB. Since very limited calibration information about the A/D converter is available, the linear approach to converter calibration which gives better results is preferred.

#### 4.0 Data Processing

Section 3.0 of this report calculated the scattering coefficient in terms of the ratio of received power to transmitted power, and then related this ratio to the measurements taken by the scat processor. The calculation is completed by detailing the steps necessary to process the raw digital measurement numbers into the desired power ratio. This power ratio is then inserted into the modified radar equation, and the scattering coefficient is computed.

---

<sup>5</sup> GE Calibration Data Report, Vol. 1A, p. 2-71.

Under the linear A/D conversion assumption, raw digital PCM counts are converted into analogue voltages. These voltages are formed by the classic D/A conversion equation:

$$V_{(analog)} = V_o \sum_{m=1}^n A_m 2^{-m} \quad (5)$$

$V_o$  = voltage weight of the MSB (2.5 volts)

$A_m$  = logical value of the  $m^{th}$  significant bit (1 or 0)

$n$  = number of magnitude bits (10)

The voltage computed by Equation (5) now represents the largest output from the three data channel integrators.

In order to reference the measurement to the input of the integrator, the dc offset and ramp error voltages must be subtracted. If the offset current and voltage ramp errors are lumped into a single constant, Equation (4) may be expressed in terms of the true average signal voltage at the input of the integrator.

$$\langle e_{in} \rangle = \left[ e_o - V_{os} - \frac{K T}{R_{in} C} \right] \frac{R_{in} C}{T} \quad (4a)$$

$$K = V_{os} + I_{os} R_{in}$$

$T$  = integration time

The measurement processing is completed by referencing the integrator input voltage to the receiver front end voltages given by Equation (3a). This is done by normalizing path differences through the attenuator steps, filter banks, and data channels. Doppler spreading effects are compensated by normalizing with respect to doppler filter bandwidth, since it was designed to be a constant multiple of expected doppler spread. This will of course introduce some error, but this error is small compared to 1db (~5% worst case). Insertion loss through each path (this includes the 10db attenuation steps) is also computed and applied to each measurement. The normalized noise measurement is now subtracted from the normalized signal plus noise measurement to derive the final refined voltage which is the best representation of average signal power.

//

Since the SCAT CAL measurement is near the top of the dynamic range of the instrument, any noise correction is insignificant. Since the SCAT CAL signal is not shifted in frequency, no correction for doppler spreading is required. Accordingly, all filter paths were normalized to the 0° Middle Center Frequency filter used for the SCAT CAL measurement. The 0° Lower Center Frequency filter was also used to take a SCAT CAL measurement, but this measurement was a check on transmitter frequency stability, and was not used in data processing.

Equations (6) and (6a) summarize the development of the "signal-plus-noise minus noise" voltage, and Equation (7) incorporates normalization corrections due to the different signal paths between the input of the 10db attenuator steps and the input to each integrator, and relates all measurement quantities to the form of Equation (3a).

$$V_s'' = \left[ V_{sn} - V_{os} - \frac{K(IT)_s}{(TC)_s} \right] \frac{(TC)_s}{(IT)_s} - \left[ V_{sn} - V_{os} - \frac{K(IT)_n}{(TC)_n} \right] \frac{(TC)_n}{(IT)_n} \quad (6)$$

$$V_s'' = \frac{V_s' (TC)_s}{(IT)_s} - \frac{V_n' (TC)_n}{(IT)_n} \quad (6a)$$

$V_{sn}$  = uncorrected raw scat signal plus noise voltage

$V_s''$  = corrected signal only voltage (time averaged)

$V_s'$  = integrator output voltage of the signal plus noise measurement  
corrected for offset voltage and current (per Equation 4a)

$V_n'$  = integrator output voltage of the noise only measurement  
corrected for offset voltage and current (per Equation 4a)

$(IT)_s$  = integration time of the signal plus noise measurement

$(IT)_n$  = integration time of the noise measurement

$(TC)_s$  = integrator  $R_{in}$  C time constant of the signal plus noise measurements

$(TC)_n$  = integrator  $R_{in}$  C time constant of the noise measurement

12

$$\frac{P_r}{P_t} = \frac{K_c}{K_r K_t} \left[ \frac{\left( \frac{V'_s (TC)_s}{A_s (IT)_s} \right) - \left( \frac{V'_n (TC)_n}{A_n (IT)_n} \right)}{\frac{V'_c (IT)_c}{A_c (TC)_c}} \right] \quad (7)$$

$A_s$  = signal path normalization for signal plus noise

$A_n$  = signal path normalization for noise only

$A_c$  = signal path normalization for calibration

$V'_c$  = calibration measurement voltage corrected for integrator effects

$(TC)_c$  = integrator  $R_{in} C$  time constant of the calibration measurement

$(IT)_c$  = integration time of the calibration measurement

Since the detection scheme used a germanium microwave mixing diode, a temperature dependence of the normalization constants was noted. Data are available which document this dependence at three distinct temperatures,<sup>6</sup> but the variation of the data points does not necessarily suggest that a linear interpolation is appropriate.<sup>7</sup> A second-order fit vs. linear interpolation shows that the difference between these two interpolation methods can approach the deviation between the nominal scat processor gain predicted by linear interpolation and the scat processor gain at the nearest temperature data point. Implementation of any temperature correction to normalization gains was therefore left to the discretion of MMC.

One final modification to Equation (7) resulted from degraded performance at 48° pitch command angles. Mechanical limitations restricted the S-193 pitch gimbal to a maximum angle of about 43°. This angle was not uniformly reached during each 48° commanded scan, and some scat signal plus noise measurements were degraded.

<sup>6</sup> GE Calibration Data Report, Vol 1A, p. 4-4A.

<sup>7</sup> Telecon Mr. V. Kaup, MMC, 06 June 1974.

13

This degradation was because the doppler shift of the return was inadequate to place the return spectrum in the passband of the 48° LCF. This problem was corrected by calculating doppler shift and fitting a fifth-order polynomial to the lower skirt of the 48° LCF. No correction was required if doppler shift exceeded 480 KHz, since this placed the return spectrum in the 48° LCF passband. No calculation was made if doppler shift were less than 440 KHz because this was outside the data range for the 48° LCF filter characteristic.

It was further assumed that the return spectrum could be approximated by an impulse for the range of doppler shifts between 440 KHz and 480 KHz. This is obviously not true, but is probably no more serious than the error introduced by the calculation of doppler shift from ephemeris data. This correction factor was erroneously applied to the normalized signal plus noise measurement in the original data processing equation. It has now been changed to correct the final representation of the signal only measurement, i. e. the entire numerator of Equation (7). Thus Equation (7) is multiplied by a variable factor (D) which depends on calculated doppler shift.

$$\frac{P_r}{P_t} = \frac{K_c}{K_r K_t} \left[ \frac{\frac{V'_s(TC)_s}{A_s(IT)_s} - \frac{V'_n(TC)_n}{A_n(IT)_n}}{\frac{V'_c(IT)_c}{A_c(TC)_c}} \right] \cdot D \quad (7a)$$

$D$  = filter attenuation correction applied for  $440 \text{ KHz} \leq \Delta f_d \leq 480 \text{ KHz}$ ,

$D = 1$  for  $\Delta f_d > 480 \text{ KHz}$

(No data processing is made for  $\Delta f_d < 440 \text{ KHz}$  @  $P = 48^\circ$ )

$\Delta f_d$  = calculated doppler center frequency shift

14



The result calculated by Equation (7a) is substituted into the expression derived from the radar equation for scattering coefficient.

## 5.0 Parameter Estimation Accuracy

The stability of the S-193 Scatterometer was well-documented in preflight testing.<sup>9</sup> Inspection of Equation (2) shows that errors in scattering coefficient may arise from errors in transmitter wavelength, range, calculation of received to transmitted power, and the illumination integral. This argument initially assumes that the simplifying assumptions which obtained Equation (2) from the more general radar Equation (1) are entirely valid. As pointed out in Section 3.1, this is both reasonable and justified.

The SCAT CAL measurement has demonstrated throughout SL-2, SL-3, and SL-4 that transmitter wavelength was an extremely stable number. Until the apparent damage to the antenna feed noted during SL-4, the illumination integrals were also expected to be stable. This does not imply that the original calculations were accurate, but rather that scattering coefficients for a given scatterometer transmit and receive polarization may be accurately compared against each other. This is evident by noting that the illumination integral in Equation (2) depends only upon polarization of transmit and receive paths. It is therefore assumed that the antenna pattern from space was close enough to the preflight data to introduce negligible error. The KU APEX results will confirm this argument.

On the other hand, there has been considerable concern over the accuracy of ephemeris data. This unfortunately represents a situation over which there is little control, but there has been no evidence to date which indicates that range error exceeds a few percent. This degree of accuracy for range would be acceptable if the ratio of received to transmitted power can be accurately determined.

---

<sup>8</sup> PHO-TR524, p. 6-20.

<sup>9</sup> GE Calibration Data Report V. 1A, S-193 Historical Logbook, KSC Engineering Baseline Report (S-193 Sensor Performance Evaluation).

An examination of Equation (7a) shows that sources of error are either due to differences in measurement signal paths or instabilities in common signal paths. What this means is that non-concurrence of the three scatterometer measurements in time necessarily implies some error in comparing them per Equation (7a). Therefore, any signal path common to all three measurements will not affect the result computed in Equation (7a) as long as its parameters are stable, e.g. gain and bandwidth of the tunnel diode amplifier in the RF oven. Absolute parameter stability need not even be repeatable from day to day or mode to mode as long as it remains stable during a given system data group. That is, it does not matter whether the tunnel diode amplifier has 30 db or 32 db of gain during a given set of data measurements as long as its gain is constant during these measurements. This argument does have limitations with respect to the dynamic range of the instrument, but it also points out a less rigorous accuracy requirement on all common signal paths.

Having discussed the reasons for generally ignoring variation in common signal paths, Equation (7a) is examined for sources of instability. Possible sources of error are receiver front-end parameters ( $K_c$ ,  $K_r$ ,  $K_t$ ), integrator parameters ( $V_s'$ ,  $V_n'$ ,  $V_c'$ , TC, IT), filter parameters ( $A_s$ ,  $A_n$ ,  $A_c$ ), and the doppler correction for  $48^\circ$  command angles (D). The factors influencing accuracy of the doppler correction factor were discussed in Section 4.0.

Stability of  $K_c$  has been determined by SCAT CAL measurement repeatability during SL-2, SL-3, and SL-4. Integrator time constant (TC) may also be assumed stable, since it is the product of two precision passive components which will remain fixed over wide environmental changes. Similar argument can be made for the stability of the 10db attenuation steps in  $A_c$ ,  $A_s$ , and  $A_n$ . All remaining factors cited from Equation (7a) have relatively unknown stability.

Even with many unknown individual parameter stabilities, the accuracy of Equation (7a) may still be checked from space data. The Lunar Cal periods during SL-2, SL-3, and SL-4 provide a massive record of measurements while the antenna was pointed into deep space. It is clear that under these conditions, a perfect instrument will measure the same normalized SCAT signals as SCAT NOISE, i.e. the numerator of Equation (7a) will vanish. By forcing these two measurements to coincide through empirical adjustment of scat noise integration time, measurement data for all modes and command angles may be checked for homogeneity.

16

Independence of these measurements for command angle and system mode implies stability of path normalization per Equation (7a). This hypothesis was originally proposed by MMC,<sup>10</sup> and the results indicate Equation (7a) is accurate to within a few percent of the ideal behavior. This becomes a negligible fraction of one decibel, and hence the dominant source of error in the data processing is the range parameter, with the illumination integral a possible secondary source of error. Neither of these terms in the data processing Equation (2) are expected to significantly degrade accuracy of the scattering coefficient. The processing of data per Equations (2) and (7a) are therefore considered to be valid and accurate measurements of radar scattering coefficient.

---

<sup>10</sup> S-193 Sensor Performance Evaluation, Sections 3.5, 10.2.